Astragalus polysaccharide alleviates asthma by modulating gut microbiota and serum metabolomics

JIE ZHANG[1*], MING GUAN[2*], SULING WU[1] and WENBIN SHENG[1]

[1]Department of Pediatrics, Hangzhou Children's Hospital, Hangzhou, Zhejiang 310014, P.R. China;
[2]Department of Otolaryngology, Affiliated Hangzhou First People's Hospital, School of Medicine,
Westlake University, Hangzhou, Zhejiang 310006, P.R. China

Abstract. The aim of the present study was to examine the effects of *Astragalus* polysaccharide (APS) on gut microbiota and serum metabolites in asthmatic mice. For this purpose, a total of 36 BALB/c female mice were selected and randomly classified into the following groups: i) The normal control group sensitized with phosphate-buffered saline; ii) the asthma group sensitized and challenged with ovalbumin (OVA); iii) the OVA + APS (2.5 g/kg) treatment group; iv) the OVA + APS (5.0 g/kg) treatment group; v) the OVA + APS (10 g/kg) treatment group; and vi) the OVA + dexamethasone (2 mg/kg) treatment group, with 6 mice in each group. OVA was used to establish the mouse model of asthma. In the APS group, the asthmatic mice were intragastrically administered APS at various doses at 1 h prior to each OVA stimulation. The airway hyperreactivity (AHR) was measured, and hematoxylin and eosin staining was employed to evaluate pulmonary inflammatory infiltration. In addition, 16S rRNA sequencing and ultra-performance liquid chromatography-tandem mass spectrometry were used to detect the changes in the mouse gut microbiota and serum metabolites. The results revealed that compared with the asthma model group, APS improved airway inflammation and eosinophil infiltration in asthmatic mice. In asthmatic mice, the gut microbial imbalance mainly manifested as a low abundance of Bacteroidetes and a high abundance of Firmicutes, yielding an increased F/B ratio. In the high-dose APS group, the abundance of Firmicutes was reduced, and the abundance of Bacteroidetes was increased, which thereby decreased the F/B ratio and corrected the gut microbial imbalance. Through blood metabolomics, 145 and 105 significantly differential metabolites were detected in the medium- and high-dose APS groups, respectively. Moreover, Kyoto Encyclopedia of Genes and Genomes pathway enrichment analysis demonstrated that the metabolic pathways in the medium-dose APS group included the biosynthesis of unsaturated fatty acids and the biosynthesis of arginine. On the other hand, the metabolic pathways enriched in high-dose APS group were the biosynthesis of unsaturated fatty acids, and pyrimidine metabolism. On the whole, the present study demonstrates that APS may regulate the gut microbiota and the metabolites to improve airway inflammation and AHR in asthmatic mice.

Introduction

Bronchial asthma refers to a chronic airway inflammatory disease, which is associated with multiple cells (including eosinophils, mast cells, T-lymphocytes, neutrophils, smooth muscle cells and airway epithelial cells) and cellular components in the human body. It is usually accompanied by airway hyperreactivity (AHR), widely variable and reversible airway limitation and symptoms, such as recurrent wheezing, dyspnea, chest distress or cough. This disease often occurs or is aggravated at night and in the early hours of the morning, and the symptoms can be relieved spontaneously or following treatment (1,2). At present, asthma is one of the relatively commonly observed chronic diseases globally, exhibiting a gradually increasing prevalence rate, and markedly affects the quality of life and physical health of patients. Thus far, inhaled corticosteroids are the most effective treatment for bronchial asthma; however, this type of treatment is associated with drug dependence and cannot achieve ideal therapeutic efficacy in some children, since it cures the symptoms and not the disease (2). Traditional Chinese medicine (TCM) has long been applied in the treatment of asthma (3); it is of immense medical value to search for more effective TCM treatments for allergic asthma.

Astragalus, a traditional Chinese herbal medicine, has been extensively adopted for the treatment of asthma. It is a component found in well-known TCM prescriptions, such as YuPingFengSan, PingChuanGuBen Decoction and modified LiuJunZi Decoction, while *Astragalus* polysaccharide (APS) is one of the primary active ingredients in *Astragalus* (4,5).

Gut microbial imbalance is the new direction of research on the occurrence and progress of asthma in children, and regulating the gut microbial composition may become an effective method for the prevention or treatment of asthma (6). Based on the TCM theories of 'the lung and the large intestine being interior-exteriorly related' and 'reinforcing earth to generate metal', modern medicine has put forth the concept of the 'lung-intestinal' axis. The present study aimed to examine the effects of APS on the gut microbiota and metabolites in asthmatic mice based on 16S rRNA and non-targeted metabolomics.

Materials and methods

Drugs and reagents. APS (purity, >98%; Shanghai Macklin Biochemical Co., Ltd.), ovalbumin (OVA) and aluminium hydroxide (Sigma-Aldrich; Merck KGaA) were used in the experiments in the present study.

Animal and experimental protocols. A total of 36 healthy female BALB/c mice (weighing 18-22 g, 4-6 weeks old) were purchased from the Laboratory Animal Center of Hangzhou Medical College. All experimental protocols involving animals were approved by the Ethics Committee of the Zhejiang Center of Laboratory Animals (Hangzhou, China; approval no. ZJCLA-IACUC-20020187) and conducted conforming to the guidelines of the China Animal Protection Commission. In addition, all mice were raised in an environment with a temperature of 22±2°C and with a relative humidity of 50±1%.

In a random manner, the 36 mice were classified into six groups, with 6 mice in each group, as follows: i) The normal control group sensitized with phosphate-buffered saline (PBS; HyClone; Cytiva); ii) the asthma group sensitized and challenged with OVA (grade V, Sigma-Aldrich; Merck KGaA); iii) the OVA + APS (2.5 g/kg) treatment group; iv) the OVA + APS (5 g/kg) treatment group; v) the OVA + APS (5 g/kg) treatment group; and vi) the OVA + dexamethasone (DXM, Sigma-Aldrich; Merck KGaA, 2 mg/kg) treatment group used as a positive control.

The establishment of the mouse model of asthma was as follows: i) The sensitization stage: The asthma model was constructed by the injection of 20 μg emulsifying OVA in 200 μl PBS on days 1, 8 and 15 of the experiment. ii) The excitation stage: Following initial sensitization, the mice were subjected to the aerosol inhalation of 1% OVA in a closed container for excitation every day from day 22, and each aerosol inhalation lasted for ~30 min for 1 week consecutively. In the negative control group, PBS was used instead of OVA during the sensitization and excitation stages. All drugs (APS and DXM) were dissolved in an equivalent amount of PBS and administered at a dose of 0.2 ml/mouse. APS was administered via intragastric administration every day for 1 week. DXM (2 mg/kg) served as the positive control and was administered in the same manner. On day 29, the enhancement suspension (Penh) was evaluated, and the mice were sacrificed on day 30. Serum, lung tissue and splenic cells were harvested for further analysis (Fig. 1). At the end of the animal experimental period, the experimental animals were subjected to cervical dislocation under anesthesia. The mice were anesthetized with 40 mg/kg pentobarbital sodium solution by intraperitoneal injection. All
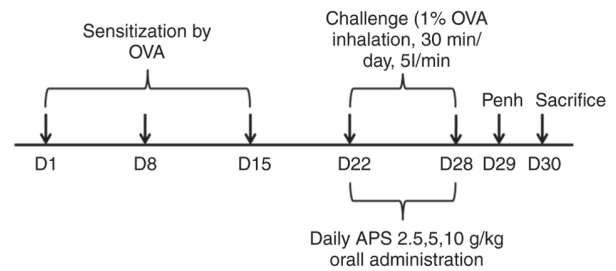

Figure 1. Schematic diagram illustrating the experimental design used for the construction of the mouse model of asthma. OVA, ovalbumin; APS, *Astragalus* polysaccharide.

procedures were carried out following strict ethical guidelines, and all efforts were made to minimize animal suffering.

Methacholine (Mch) measurement by AHR. At 24 h following the final excitation, AHR was indirectly assessed using whole-body plethysmography. More specifically, each conscious mouse was stimulated with Mch at elevating doses (Mch aerosol containing 3.125, 6.25, 12.5, 25, 5 and 50 mg/ml saline) for 3 min. The 3-min Penh value following each Mch excitation was calculated.

Hematoxylin and eosin (H&E) staining of lung tissue for histological examination. Following collection, the lung tissue was fixed with a concentration of 4% paraformaldehyde (20°C, 48 h), paraffin-imbedded and subjected to histological staining. Briefly, the 4-μm-thick left lung sections were stained with H&E (Beijing Solarbio Science & Technology Co., Ltd.; 20°C, 30 min) to evaluate eosinophil infiltration and inflammatory cell infiltration in the surrounding lung tissue.

16S rDNA sequencing analysis of gut microbiota. DNA was extracted from the mouse feces, and cellular DNA was amplified using PCR. In brief, the amplification region was bacterial 16SV3+V4, and the primers used were 338F and 806R. The V3 upstream primer sequence was 5'-ACTCCT ACGGGAGGCAGCA-3', and the V4 downstream primer sequence was 5'-GGACTACHVGGGTWTCTAAT-3'. The DNBseq sequencing process and method were applied in sequencing. In addition, the raw data were spliced with FLASH (version 1.2.11), and the spliced Tags were clustered into operational taxonomic units (OTUs) with the application of USEARCH software (v7.0.1090).

Mouse serum non-targeted metabolomics detection. An appropriate amount of serum sample was supplemented with 200 μl water for homogenization, followed by vortexing for 60 sec. Thereafter, 800 μl methanol-acetonitrile solution (1:1, Merck, V:V) was supplemented for vortexing for a further 60 sec, followed by low-temperature ultrasonic treatment twice (30 min each). After being allowed to stand at -20°C for 1 h to precipitate the protein, the sample was subject to centrifugation at 14,000 x g and 4°C for 20 min to collect the supernatant. Subsequently, the sample was separated with the ACQUITY UPLC BEH Amide chromatographic column (100x2.1 mm, 1.7 μm) of the Agilent 1290 Infinity LC ultra-performance liquid chromatography system (UPLC), and mass spectrometry
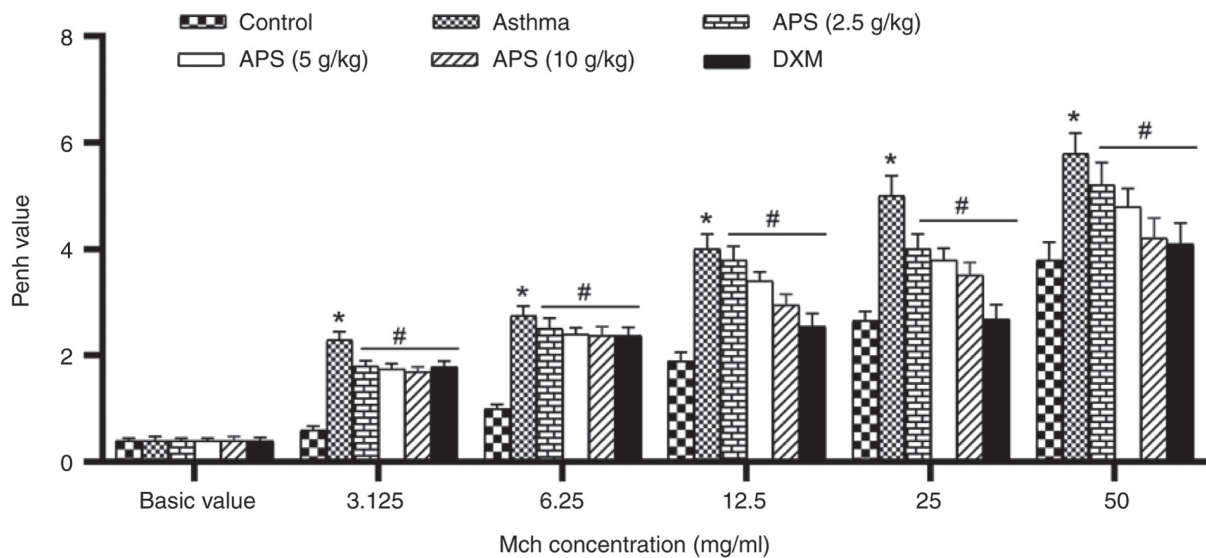
Figure 2. Effects on airway hyperreactivity. The Penh value indicates the airway hyperreactivity. Data are expressed as the mean ± standard deviation. *P<0.05, compared with the control group; #P<0.05, compared with the asthma group. APS, *Astragalus* polysaccharide; DXM, dexamethasone.

was carried out using the Agilent 6550 mass spectrometer (Agilent Technologies, Inc.). In addition, the metabolites were detected with the AB Triple TOF 6600 mass spectrometer, and the structural identification of metabolites was completed by collecting the first-order and second-order spectra of quality control (QC) samples. Following data preprocessing with Pareto scaling, unidimensional and multidimensional statistical analyses were performed, and the volcano plot was drawn using R software.

Kyoto Encyclopedia of Genes and Genomes (KEGG) metabolic pathway enrichment. Based on the KEGG compound database, the metabolites were annotated. Furthermore, the annotated metabolites were then matched based on the KEGG pathway database. Significantly regulated metabolites were imported into the metabolite enrichment analysis MetaboAnalyst 5.0 for their metabolic pathway enrichment. The enrichment results were calculated for the significance (P-values) by hypergeometric tests and presented as bubble plots.

Statistical analysis. Statistical analysis was conducted using SPSS version 22.0 software (IBM Corp.). Measurement data are presented as the mean ± standard deviation (SD) and were compared using one-way analysis of variance for comparisons among multiple groups. In pairwise comparisons, the least significant difference (LSD) test was adopted in the case of homogeneity of variance. One-way ANOVA was used for comparison between multiple groups and pairwise comparisons were conducted using the Bonferroni method. Tamhane's T2 test was used for multiple comparisons in the case of heterogeneity of variance. A value of P<0.05 was considered to indicate a statistically significant difference.

Results

Effects of APS on alleviating AHR in the bodies of mice. With the purpose of evaluating the effects of APS on AHR, the Penh values induced with various doses of Mch (3.125, 6.25, 12.5, 25 and 50 mg/ml) were measured. The AHR level in each group increased with the increase in the inhaled Mch concentration. The AHR in the asthma group was markedly higher than that in the normal control group following induction with Mch (P<0.05). However, the Penh value decreased following treatment with APS and DXM (P<0.05; Fig. 2).

Ameliorative effects of APS on airway inflammation and eosinophil infiltration in asthmatic mice. The H&E staining of mouse lung tissue revealed a large amount of inflammatory cell infiltration in the peribronchial area, such as eosinophils, neutrophils and lymphocytes (Fig. 3), with eosinophils being more prominent. Following treatment with APS, inflammatory cell infiltration markedly declined.

Effects of APS on gut microbiota in asthmatic mice. In the present study, the rarefaction curve tended to be flat, suggesting the reasonable sequencing data volume, which indirectly reflected the species richness. The Shannon curve also tended to be flat, suggesting a sufficiently large sequencing data volume (Fig. 4).

Alpha diversity of the gut microbiota in the different groups. In the present study, the sequencing depth index coverage value of each sample was >0.996, suggesting that the experimental data could truly reflect the microbial communities of the experimental samples. Alpha diversity indicates the species evenness and richness, mainly including the ACE, Chao, Shannon and Simpson indexes. As shown in Table I, compared with the control group, the OTU number of gut microbiota in the asthma group was markedly decreased (P<0.05), and the ACE, Chao and Shannon indexes exhibited a significant decrease (P<0.05). Compared with the asthma group, the OTU numbers in the APS (5.0 and 10 g/kg) groups were notably increased (P<0.05), and the ACE, Chao and Shannon indexes were also significantly elevated (P<0.05), which tended to be similar to the levels in the control group. These results
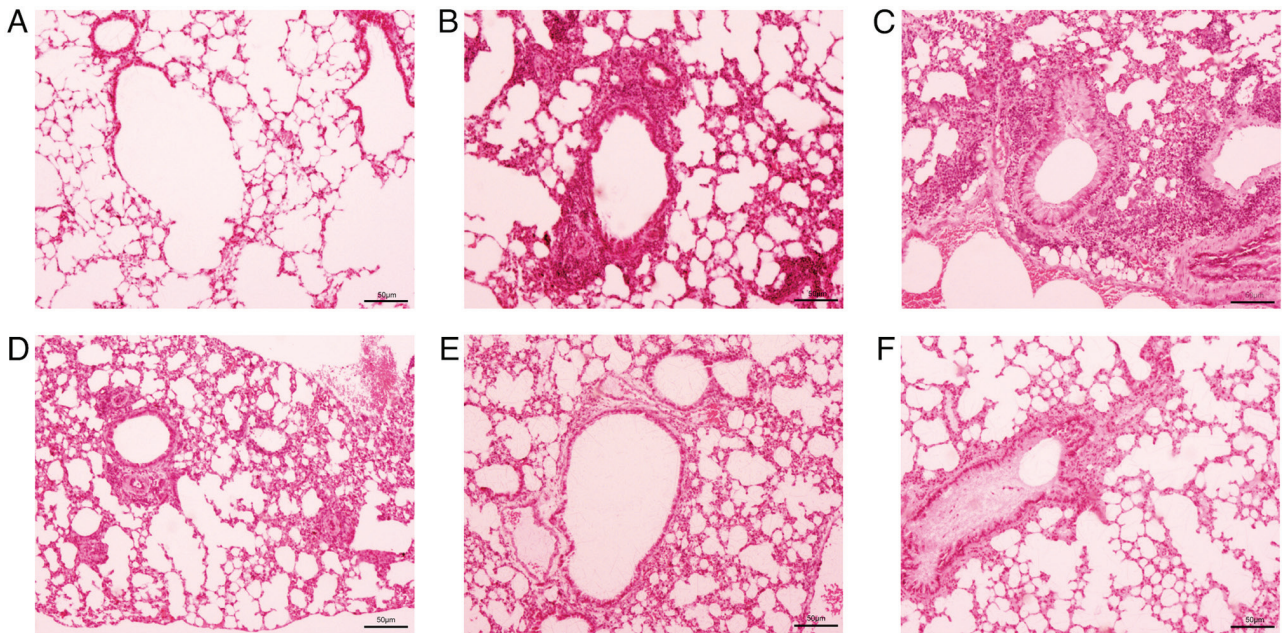
Figure 3. Effects of APS on airway inflammation. Hematoxylin and eosin staining of lung tissue (x200 magnification). (A) Normal control group, (B) asthma group, (C) APS (2.5 g/kg) group, (D) APS (5.0 g/kg) group, (E) APS (10.0 g/kg) group, and (F) dexamethasone group. APS, *Astragalus* polysaccharide.
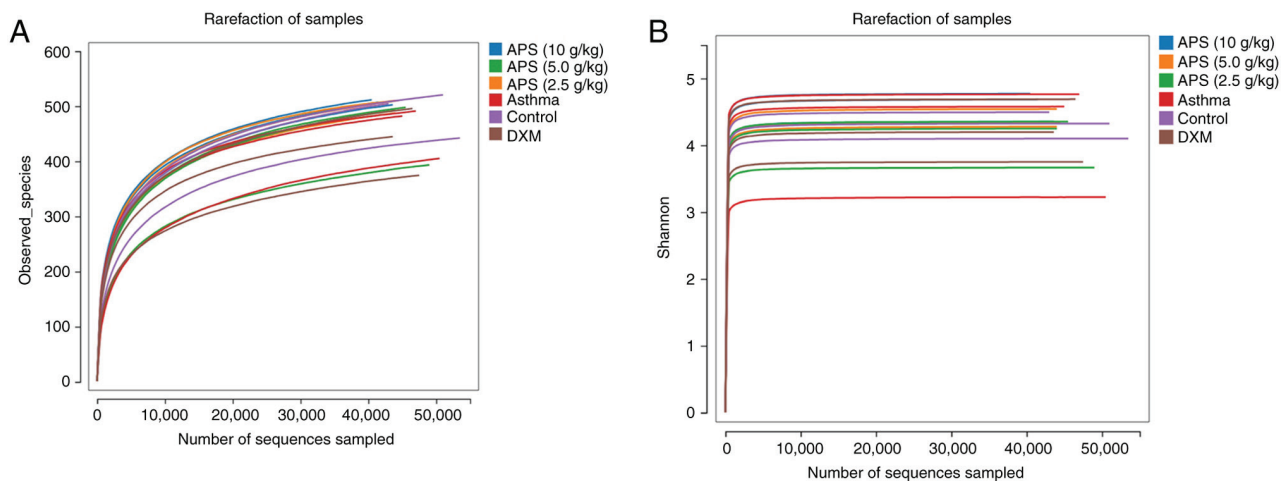

Figure 4. (A) Operational taxonomic unit rarefaction curve and (B) Shannon index curve of the samples. APS, *Astragalus* polysaccharide; DXM, dexamethasone.

suggested a marked difference in the gut microbiota between the asthmatic and normal mice, following medium- and high-dose APS intervention. In addition, the OTU numbers and alpha diversity indexes in the gut microbiota of the asthmatic mice were increased, and the microbial community abundances were recovered.

Beta diversity analysis of the gut microbiota in each group. As indicated by principal coordinates analysis (PCoA), the sample distance was the farthest between the model and control group, and these two groups were well distinguished, revealing the obvious difference in community structure between the two groups (Fig. 5). In other words, the gut microbial communities in the asthmatic mice were markedly altered. By contrast, the sample distribution in the high-dose APS group gradually approached the level in the normal group, and exhibited

intersection with the latter. In particular, the high-dose APS group was the closest to the normal group, suggesting that APS regulated the gut microbial communities in asthmatic mice and alleviated asthma-induced dysbacteriosis.

Gut microbial species composition and differential analysis in each group
Analysis of gut microbial species structure at the phylum level. As illustrated in Fig. 6, at the phylum level, the gut microbiota in the mice primarily consisted of Firmicutes, Proteobacteria, Bacteroidetes and Actinoidetes, among which, Firmicutes and Bacteroidetes were the dominant bacterial communities. Compared with the control group, the relative abundance of Firmicutes in the model group was elevated by 16.5%; compared with the model group, the relative abundances of Firmicutes in the three APS groups (2.5, 5.0 and 10 g/kg) decreased by

Table I. Alpha diversity index comparison based on the total number of OTUs.

Group	No. of mice	OTU	Chao	ACE	Shannon	Simpson
Control	6	489.67±22.64	542.45±21.25	539.83±19.76	4.31±0.06	0.04±0.008
Asthma	6	460.33±12.59[a]	518.34±15.05[a]	510.94±18.07[a]	4.19±0.087[a]	0.05±0.019
APS (2.5 g/kg)	6	461.67±47.89[b]	512.38±42.64[b]	512.45±44.79[b]	4.09±0.37[b]	0.05±0.017
APS (5.0 g/kg)	6	503.33±10.84[b]	554.75±14.85[b]	547.89±9.91[b]	4.39±0.11[b]	0.04±0.006
APS (10 g/kg)	6	507.67±3.68[b]	554.33±4.92[b]	555.96±3.92[b]	4.61±0.18[b]	0.05±0.008
DXM	6	438.67±49.60[b]	486.02±45.53[b]	484.06±47.99[b]	4.21±0.38[b]	0.04±0.019

OTUs, operational taxonomic units; APS, *Astragalus* polysaccharide; DXM, dexamethasone. [a]$P<0.05$ vs. control group; [b]$P<0.05$ vs. asthma group.
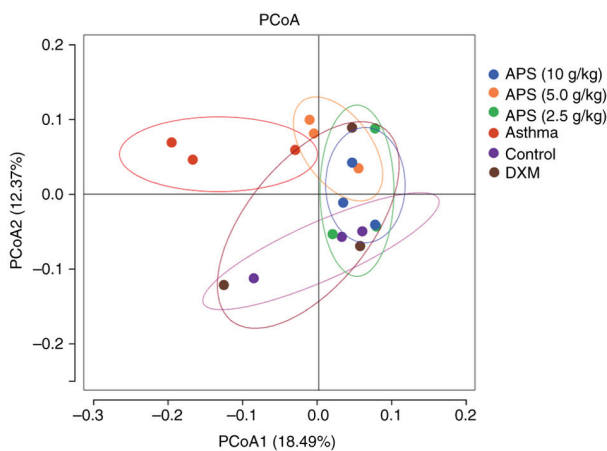

Figure 5. PCoA of beta diversity of mouse gut microbiota. PCoA, principal co-ordinates analysis. APS, *Astragalus* polysaccharide; DXM, dexamethasone.

0.21, 7.9 and 14.5%, respectively. Compared with the normal control group, the relative abundance of Bacteroidetes was reduced by 8.9% in the model group. Compared with the model group, the relative abundance of Bacteroidetes in the APS (2.5 g/kg) group decreased by 3.2%, while the abundance in the other APS (5.0 and 10 g/kg) groups was elevated by 8.4 and 12.3%, respectively. The Firmicutes/Bacteroidetes (F/B) ratio is usually used as a marker to evaluate gut microbial disturbance (7). In asthmatic mice, the gut microbial imbalance mainly manifested as a low abundance of Bacteroidetes and a high abundance of Firmicutes, yielding an increased F/B ratio. When compared with the control group, the F/B ratio in the model group tended to significantly increase. Compared with the model group, the F/B ratios in the APS (5.0 and 10 g/kg) groups exhibited a decreasing trend. In the high-dose APS group, the abundance of Firmicutes decreased, and that of Bacteroidetes increased, thereby decreasing the F/B ratio and correcting the gut microbial imbalance (Table SI).

Analysis of gut microbial species structure at the genus level. As demonstrated in Fig. 7, compared with the normal control group, the relative abundances of *Lactobacillus*, *Prevotella*, *Helicobacter* and *Barnesiella* were decreased in the model group, while those of *Alistipes* and *Clostridium_*XlVa were increased. Compared with the model group, the abundances of *Lactobacillus*, *Barnesiella* and *Prevotella* in the fecal samples of mice in the APS (5.0 and 10 g/kg) groups were increased, while the abundance of *Clostridium_*XlVa was decreased (Table SII). These findings indicated the positive regulatory effects of APS on gut microbial communities in asthmatic mice at the genus level. More specifically, APS increased the abundances of probiotics and suppressed the growth of pernicious bacteria.

Serum metabolomics analysis in asthmatic mice treated with APS

Differential metabolites in mouse serum samples. As shown in Fig. 8, in the partial least squares-discriminant analysis (PLS-DA) model, the model group was notably distinguished from the other groups, indicating that the occurrence of asthma and the interventions of low-, medium- and high-dose APS treatment markedly altered the intestinal metabolite concentrations in the mice. Combined with fold change (FC) analysis and the t-test, the significance in the changes of metabolites between two samples was analyzed and visualized in the form of a volcano plot (Fig. 8). In the volcano plot, red and blue points indicated metabolites of FC>1.5 and P<0.05, namely, the differential metabolites between two groups, with red points indicating significantly upregulated, whereas blue points represented significantly downregulated metabolites. In the present study, significantly up- and downregulated differential metabolites were found between the model and control groups (Fig. 8A), the model group and low-dose APS group (Fig. 8B), the model group and medium-dose APS group (Fig. 8C), the model group and high-dose APS group (Fig. 8D), as well as between the model group and DXM group (Fig. 8E). Further hierarchical clustering suggested that there were 145 differential metabolites between the model group and APS (5.0 g/kg) group, including the significantly upregulated 3-hydroxyhexanoylcarnitine, N-palmitolenoyltaurine, 1-palmitoleoylglycero and 3-hydroxybutyrylcarnitine, as well as the significantly downregulated glycylvaline, S-adenosylhomocysteine and 5-methyl-2'-deoxycytidine (Fig. 9A).

Upon further hierarchical clustering, 105 significant differential metabolites were detected between the model group and APS (10 g/kg) group, including the significantly upregulated cholate, 7-ketodeoxycholate and ursocholate, together with the significantly downregulated glycitein sulfate, pinitol, glycylvaline, dihomo-linolenoyl-choline, catechol glucuronide,
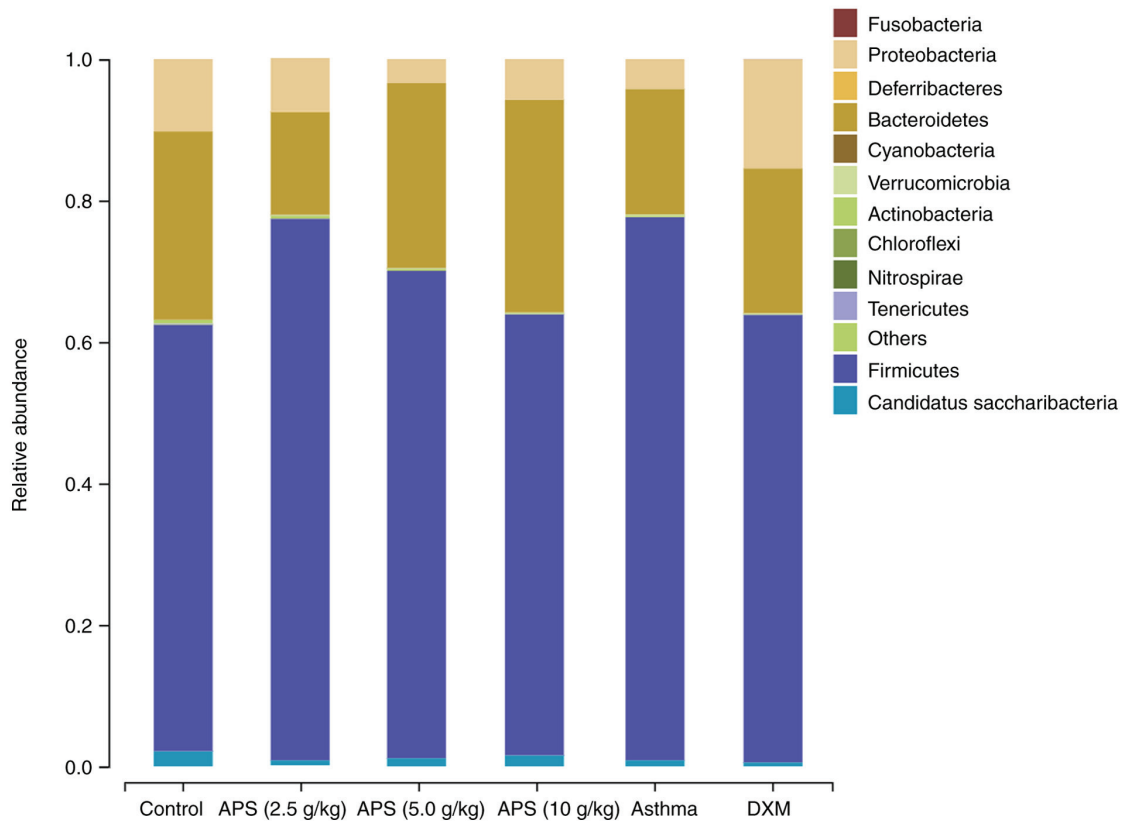
Figure 6. Histogram illustrating the mouse gut microbial community structure at the phylum level. 'Others' indicates other unidentified bacteria. APS, *Astragalus* polysaccharide; DXM, dexamethasone.
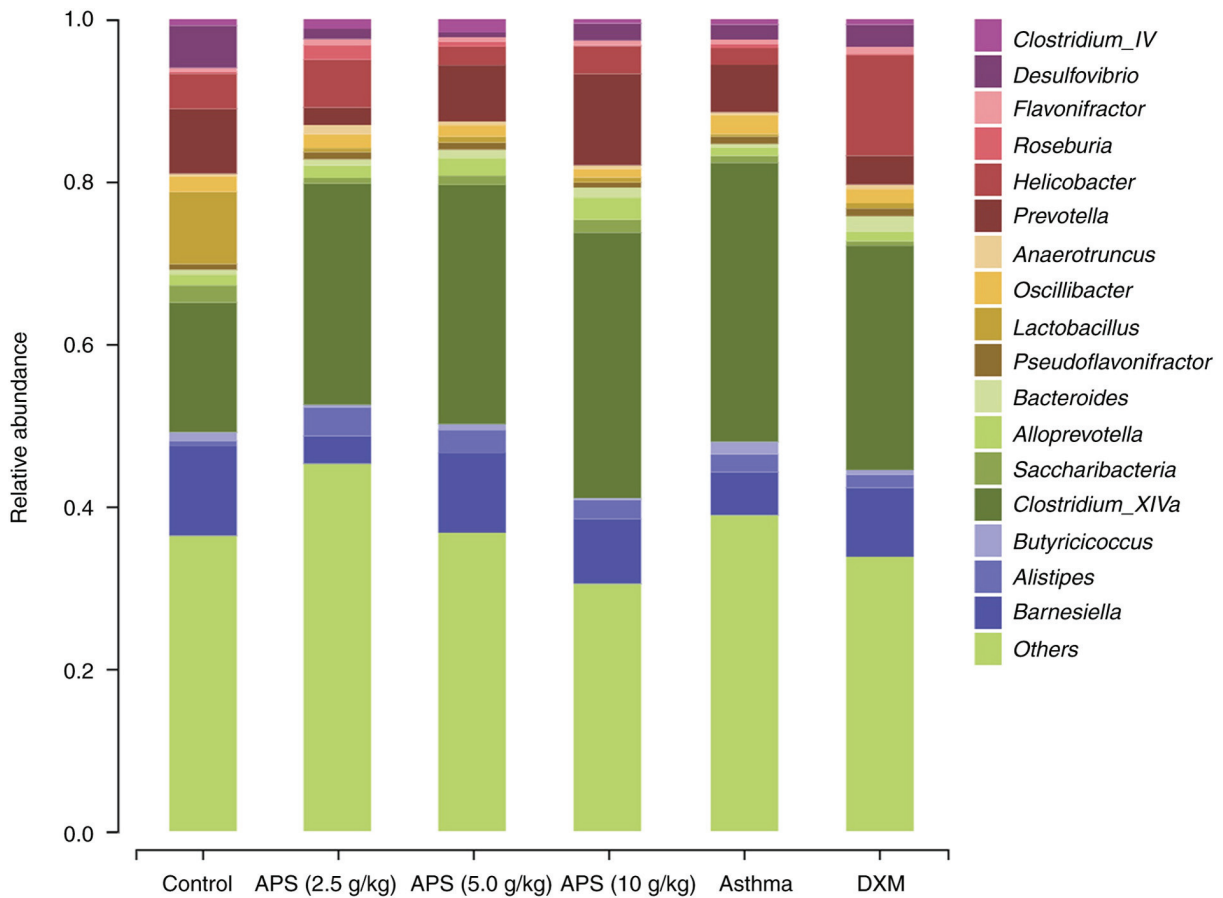
Figure 7. Histogram illustrating the mouse gut microbial community structure at the genus level. APS, *Astragalus* polysaccharide; DXM, dexamethasone.
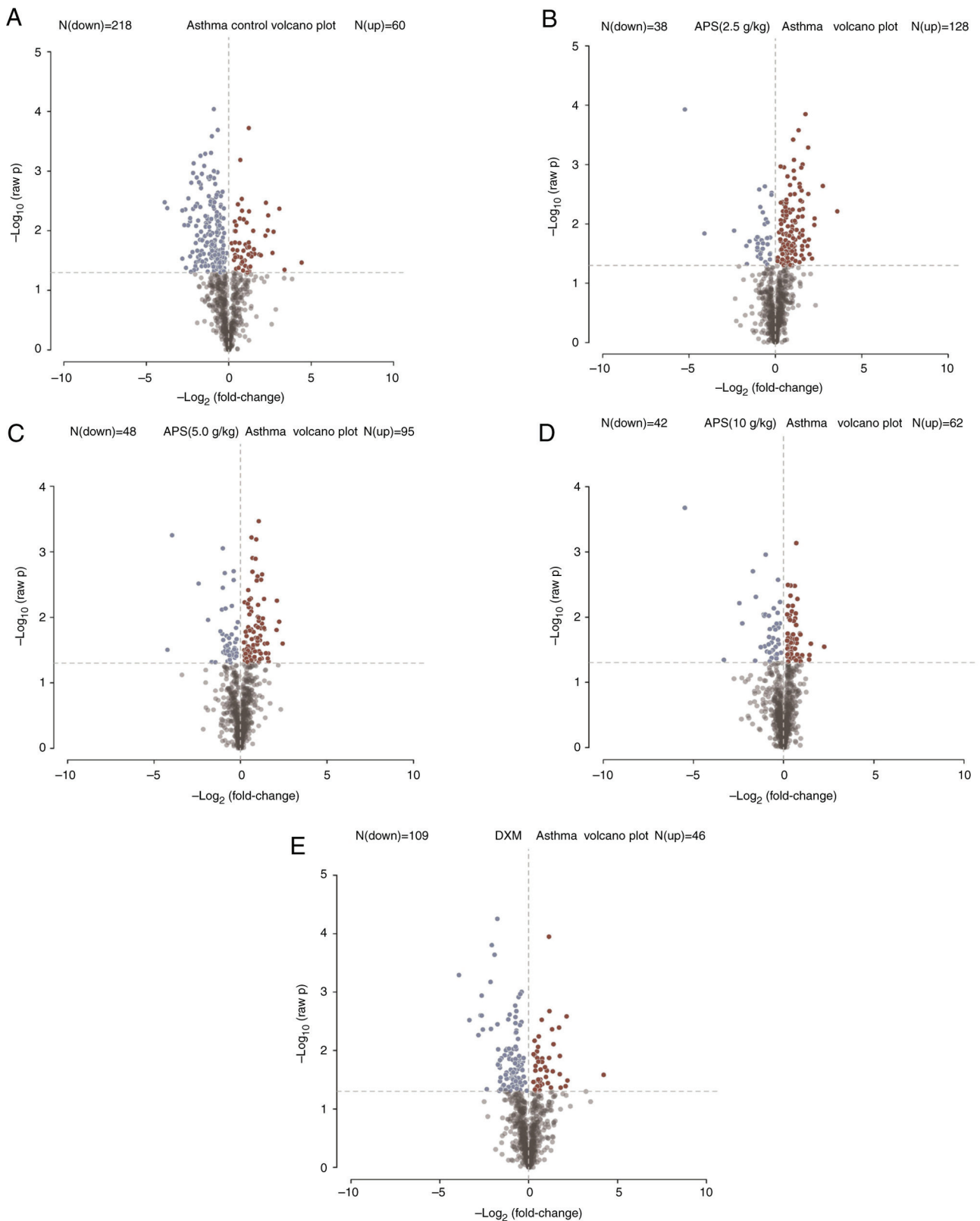
Figure 8. Significance of metabolites between two samples analyzed by variance analysis and the t-test to generate a volcano plot. (A) Model group and control group, (B) model group and low-dose APS group, (C) model group and medium-dose APS group, (D) model group and high-dose APS group, (E) model group and DXM group. Red indicates significant upregulation, whereas blue represented significant downregulation. APS, *Astragalus* polysaccharide; DXM, dexamethasone.

3-(3-hydroxyphenyl)propionate sulfate and ursodeoxycholate. These results revealed that APS could alter the blood metabolites in mice (Fig. 9B).

Analysis of related metabolic pathways. As presented in Fig. 10, KEGG pathway enrichment analysis suggested that the most significantly affected metabolic pathways in the

A

APS(5.0 g/kg) vs Asthma

Group
- APS(5.0g/kg)
- Asthma

Group
1.3
1.2
1.1
1
0.9
0.8

7-ketodeoxycholate
catechol glucuronide
1,2-dipalmitoyl-GPE (16:0/16:0)*
3-hydroxyhexanoylcarnitine (1)
N-palmitoleoyltaurine*
3-hydroxyoctanoylcarnitine (1)
1-palmitoleoylglycerol (16:1)*
3-hydroxybutyrylcarnitine (2)
2,4-di-tert-butylphenol
2-hydroxypalmitate
1-arachidonoyl-GPI (20:4)*
docosahexaenoate (DHA; 22:6n3)
palmitoyl ethanolamide
1-stearoyl-2-oleoyl-GPG (18:0/18:1)
1-stearoyl-2-oleoyl-GPC (18:0/18:1)
N,N-dimethyl-pro-pro
N-acetyltaurine
1-palmitoyl-2-dihomo-linolenoyl-GPC (16:0/20:3n3 or 6)*
galactonate
adrenate (22:4n6)
sedoheptulose
indole-3-carboxylate
lignoceroylcarnitine (C24)*
mannitol/sorbitol
stearate (18:0)
1-linoleoyl-2-linolenoyl-GPC (18:2/18:3)*
linoleate (18:2n6)
1-oleoyl-2-linoleoyl-GPC (18:1/18:2)*
palmitate (16:0)
orotidine
2-hydroxystearate
arachidonate (20:4n6)
1-linolenoyl-GPC (18:3)*
sulfate*
1-stearoyl-GPC (18:0)
19,20-DiHDPA
octadecenoate
N6-carboxymethyllysine
5-methylcytidine
linolenate [alpha or gamma; (18:3n3 or 6)]
stearidonate (18:4n3)
10-heptadecenoate (17:1n7)
dihomo-linoleate (20:2n6)
dihomo-linolenate (20:3n3 or n6)
docosapentaenoate (n3 DPA; 22:5n3)
heneicosapentaenoate (21:5n3)
arachidate (20:0)
margarate (17:0)
12-HEPE
14-HDoHE/17-HDoHE
1,2-dilinoleoyl-GPC (18:2/18:2)
1-palmitoyl-2-stearoyl-GPC (16:0/18:0)
N-lactoyl phenylalanine
14,15-DiHETrE
ribitol
thyroxine
trimethylamine N-oxide
glycerophosphoethanolamine
chiro-inositol
4-guanidinobutanoate
pyridoxate
docosapentaenoate (n6 DPA; 22:5n6)
oleoyl-arachidonoyl-glycerol (18:1/20:4) [2]*
methyl glucopyranoside (alpha + beta)
acetylcarnitine (C2)
indolepropionylglycine
glycerol 3-phosphate
palmitoleate (16:1n7)
oleoyl-linoleoyl-glycerol (18:1/18:2) [1]
1-linolenoylglycerol (18:3)
1-linoleoylglycerol (18:2)
eicosapentaenoate (EPA; 20:5n3)
corticosterone/cortexolone
cinnamate
arachidonoyl ethanolamide
heptadecatrienoate (17:3)*
1-oleoylglycerol (18:1)
1-dihomo-linolenylglycerol (20:3)
docosatrienoate (22:3n3)
indolepropionate
indoleacrylate
nisinate (24:6n3)
hippurate
2,6-dihydroxybenzoic acid
4-HDoHE
mead acid (20:3n9)
pinitol
N-palmitoyl-sphinganine (d18:0/16:0)
N-acetylhomocitrulline
N-palmitoyl-phytosphingosine (t18:0/16:0)
3-phenylpropionate (hydrocinnamate)
2-aminophenol sulfate
glycitein sulfate (2)
3-methoxycatechol sulfate (2)
4-methoxyphenol sulfate
nicotinamide riboside
quinate
glycylvaline
ursodeoxycholate
ursocholate
2-oxindole-3-acetate
beta-muricholate
indoleacetylglycine
isocaproylglycine
2S,3R-dihydroxybutyrate
3-hydroxyoctanoylglycine
glycine conjugate of C6H10O2 (2)**
ascorbic acid 2-sulfate
sebacate (C10-DC)
1-palmitoyl-2-arachidonoyl-GPE (16:0/20:4)*
1-stearoyl-2-docosahexaenoyl-GPE (18:0/22:6)*
3-hydroxy-2-ethylpropionate
bilirubin (E,E)*
gamma-glutamylglycine
glycine conjugate of C6H10O2 (3)**
thymidine
2'-deoxyuridine
N-methylproline
1-palmitoyl-2-docosahexaenoyl-GPE (16:0/22:6)*
2,3-dihydroxyisovalerate
allantoic acid
2-ketogulonate
gulonate*
allantoin
mevalonate
carnitine
2'-deoxycytidine
adenine
anserine
carnosine
glucuronate
N-acetylaspartate (NAA)
threonate
pyridoxal
1,5-anhydroglucitol (1,5-AG)
orotate
2-hydroxysebacate
3-aminoisobutyrate
heptanoyl glycine
azelate (C9-DC)
1-palmitoyl-2-linoleoyl-GPE (16:0/18:2)
6-oxopiperidine-2-carboxylate
N-formylmethionine
S-adenosylhomocysteine (SAH)
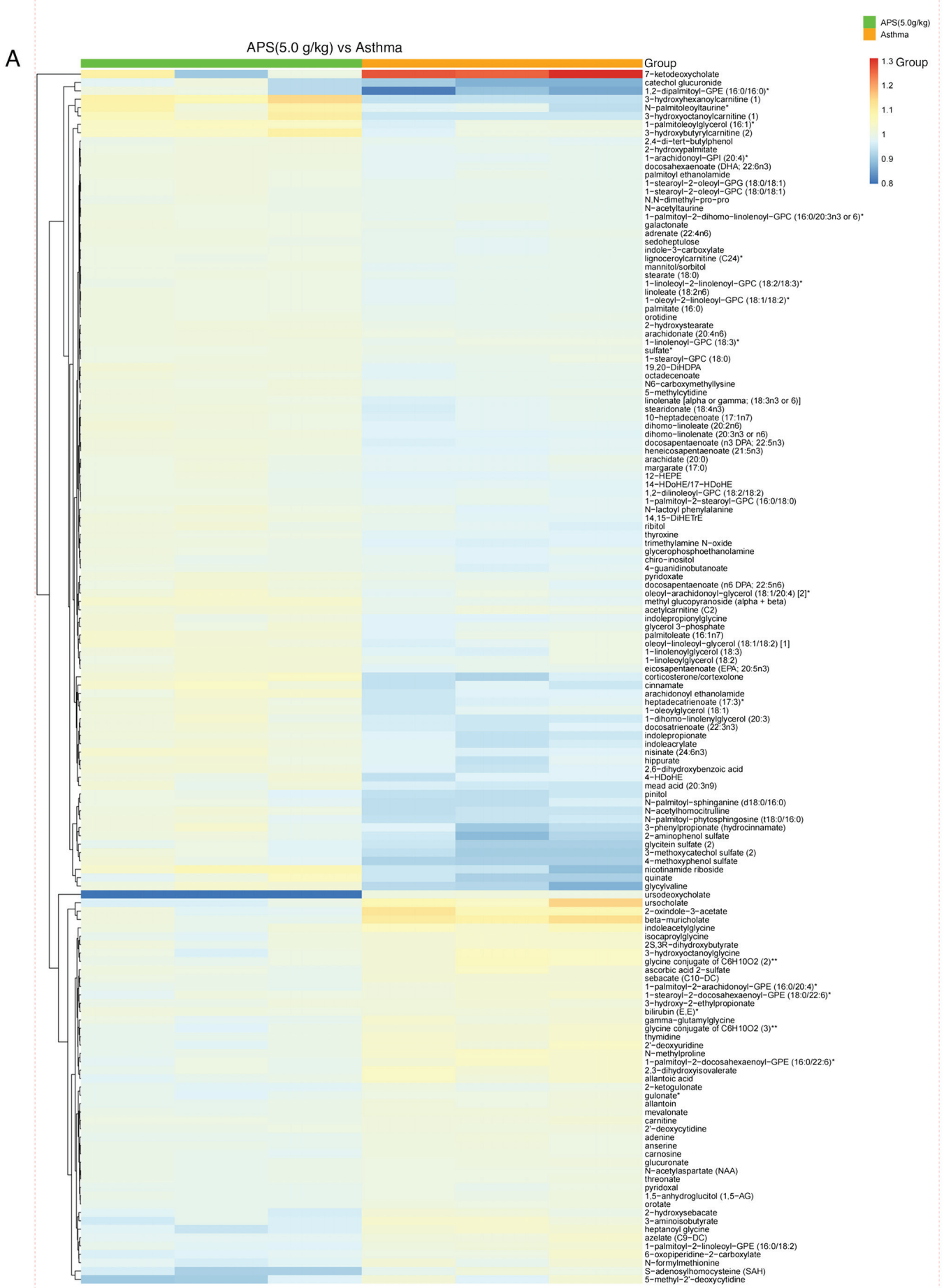5-methyl-2'-deoxycytidine

Figure 9. Continued.

Figure 9. Hierarchical clustering analysis of significant differential metabolites. (A) Model group and medium-dose APS group, (B) model group and high-dose APS group. APS, *Astragalus* polysaccharide.

model group and APS (5.0 g/kg) group were Biosynthesis of unsaturated fatty acids and Arginine biosynthesis (Fig. 10A), while those in the model group and APS (10 g/kg) group were Biosynthesis of unsaturated fatty acids and Pyrimidine metabolism (Fig. 10B).

Discussion

Based on the TCM theories of 'the lung and the large intestine being interior-exteriorly related and reinforcing earth to generate metal', modern medicine has put forth the concept of the 'lung-intestine' axis. This term refers to the microbial communities that colonize these two organs and serve as the link to form a bidirectional axis that connects the lung and the

intestine. The gut microbiota influences the occurrence and development of lung diseases. In addition, microbial disturbance induced by lung diseases, particularly allergic disease, affects the gastrointestinal tract through immunoregulation (8). The gut microbiota is considered the largest immune organ in the human body, which involves ~1,000 resident bacteria, a figure that is 10-fold that in normal human cells. Moreover, it contains genes in numbers that are 150-fold higher than those in the human body; the total microorganism amount in the gut microbiota reaches 10^{14}, and is thereby known as the second largest human genome. Gut microbial diversity is the foundation for the promotion of nutrient absorption, and maintaining body immunity and metabolism. Moreover, the changes in microbial community structure, species and functions, and
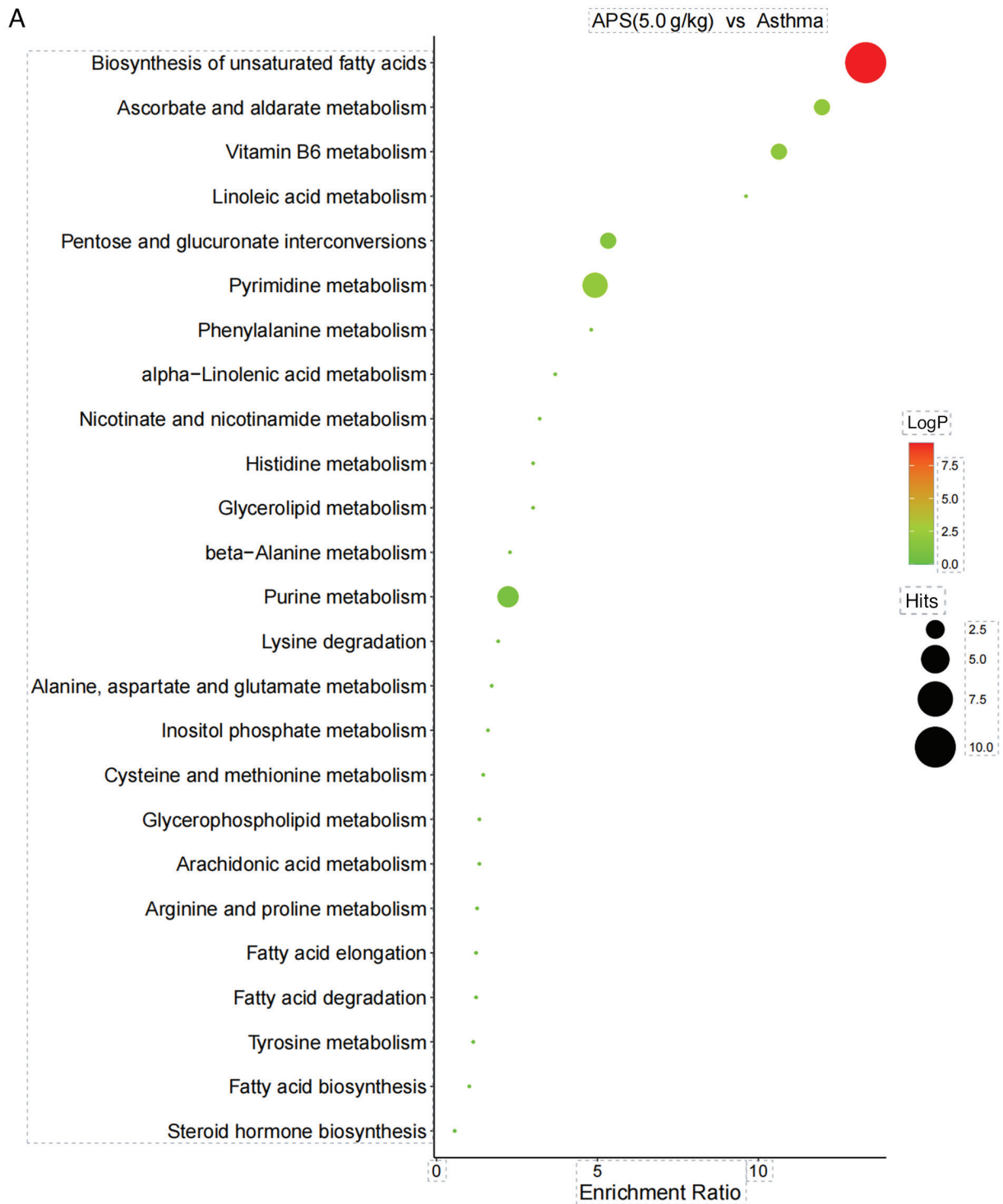
A

Figure 10. Continued.

the produced metabolites play a crucial role in improving asthma (9,10).

The gut microbiota participates in the occurrence and progression of allergic disease. A previous study collected the urine and feces samples from 319 infants at the ages of 3 months and 1 year, and recorded their health condition at the ages of 1, 3 and 5 years. In addition, that study detected the gut microbial levels in the samples through high-throughput gene sequencing and discovered that infants lacking four gut microbial communities exhibited early asthma symptoms when they were 1 year old (11,12). Regulating the gut microbial composition may become an effective method for the prevention or treatment of asthma. The application of antibiotics induces alterations in the gut microbiota, finally increasing Th2 cell-induced asthma. Consequently, maintaining a certain amount or certain species of gut microbial communities plays an indispensable role in the effects of regulatory T-cells on preventing hypersensitivity (13). The substantial role of probiotics in the treatment of allergic inflammatory disease has been verified. Probiotics can colonize the intestine and affect lung
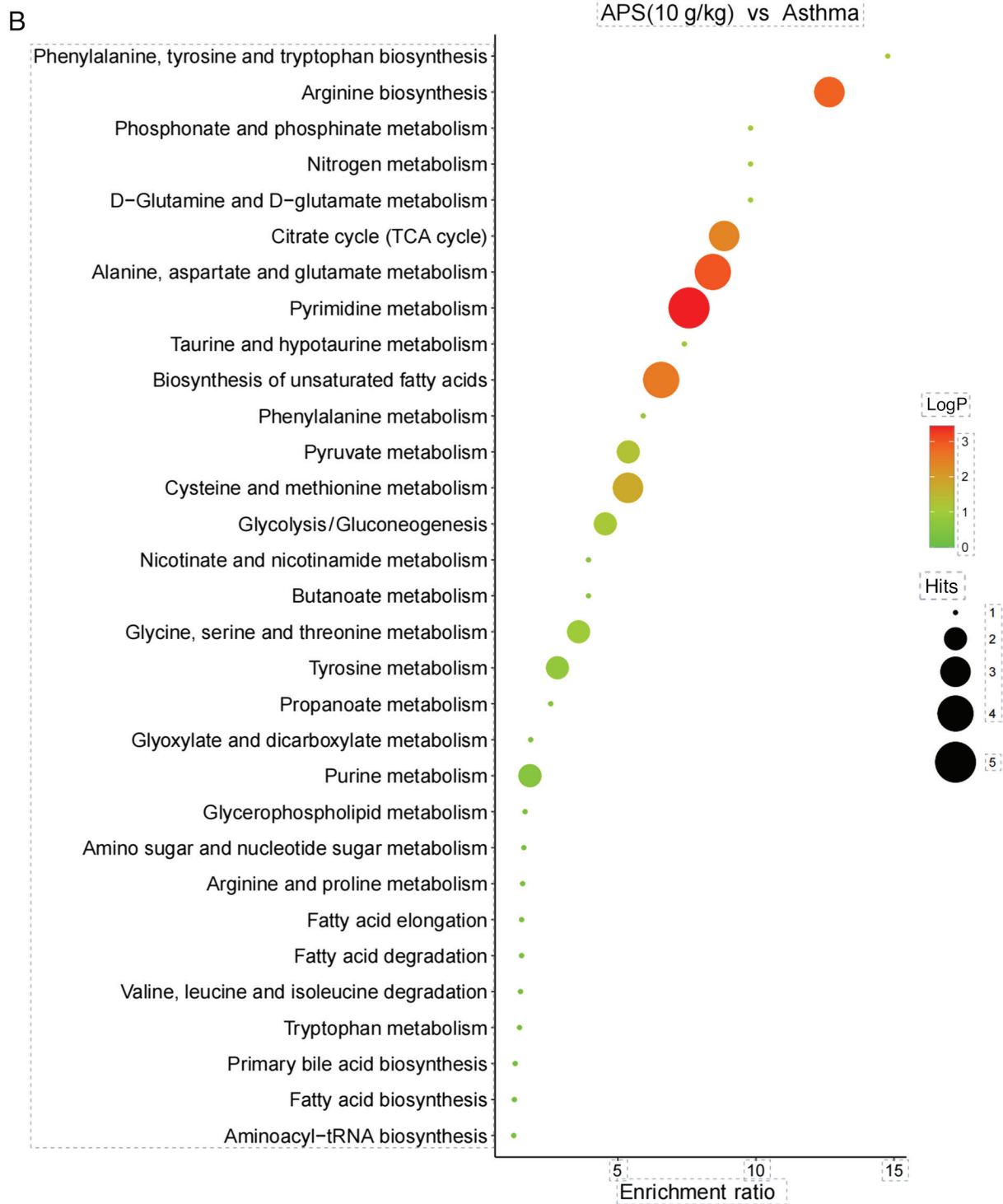
Figure 10. Kyoto Encyclopedia of Genes and Genomes pathway enrichment analysis of differential metabolites. (A) Model group and medium-dose APS group, (B) model group and high-dose APS group. APS, *Astragalus* polysaccharide.

immune function by affecting the lung microbial communities via the lung-intestine axis; therefore, this has a certain therapeutic effect on asthma (14,15). However, some studies have demonstrated that probiotics are ineffective (14,15). Thus, it may not be practical to adjust the gut microbiota composition using probiotic preparations alone. Research has indicated that increasing the Bacteroidetes abundance can decompose the carbohydrates in plants into prebiotics to alleviate inflammation. The decrease in the F/B ratio directly affects the

metabolism of dietary fiber by gut microbiota, and enhances the concentration of short-chain fatty acids (SCFAs). SCFAs can induce the production and differentiation of regulatory T-cells in the intestine; as a result, they stimulate the generation of the anti-inflammatory IL-10 level and exert a critical regulatory effect on the asthma-related metabolic disturbance via anti-inflammatory effects (16-18). In the present study, the gut microbial abundance, evenness and diversity in asthmatic mice was markedly decreased, verifying that the occurrence

and development of asthma in mice were accompanied by gut microbial alteration. Medium- and high-dose APS intervention increased the OTU number and alpha diversity indexes of the gut microbiota in mice, and restored the microbial communities, suggesting that APS improved the gut microbial imbalance in asthmatic mice. At the phylum level, medium- and high-dose APS reduced the relative abundance of Firmicutes, increased that of Bacteroidetes, reduced the F/B ratio, and corrected the alterations in the gut microbiota. Moreover, APS increased the probiotics quantities (such as *Lactobacillus*, *Barnesiella* and *Prevotella*), suppressed the growth of pernicious bacteria (such as *Clostridium*_XlVa) and exerted certain protective effects on the intestinal mucosal barrier. Thus, it can by hypothesized that APS plays a key regulatory role in the composition of the gut microbiota, which can increase the growth of probiotics, suppress pernicious bacterial growth, and thereby restrain the chronic inflammation. APS can regulate the gut microbiota, thereby increasing the content of SCFA contents, which can be absorbed directly into the blood through the intestine; APS can also regulate the changes in serum metabolic pathways caused by asthma, including biosynthesis of unsaturated fatty acids.

The concept of metabolomics was first proposed by English scholars in 1999, which is another emerging and rapidly developing bioscience after genomics and proteomics. It has a tremendous application potential in illustrating the pathogenic mechanism in the body and identifying biomarkers for diseases (19,20). Metabolomics can analyze the changes in endogenous small molecular compounds (relative molecular weight <1,000), which exist in body fluids (blood and urine), cells and tissue, at the cellular level within a short period of time (21,22). Compared with genomics and proteomics, the species of metabolites are far less than genes and proteins, and thus less data need to be processed. Metabolites are the final downstream products of transcription and translation, which are considered as the very terminal of bioinformation transfer. It is considered that 'genomics and proteomics tell you what may occur, while metabolomics tell you what actually happens' (23). According to the findings of the present study, the regulatory effects of APS on the metabolites of asthmatic mice mainly focused on the Biosynthesis of unsaturated fatty acids, the Biosynthesis of arginine and Pyrimidine metabolism. However, certain limitations should be noted in the present study. The experimental sample size was small, and thus, larger-scale experimental samples are required in the future to verify and explain the association between APS and gut microbiota, as well as metabolites. In addition, the precise mechanism of APS in affecting the gut microbiota and whether APS induces pathophysiological changes in other systems remain to be further explored, which is a future research direction.

APS, which has long been applied as a critical ingredient derived from *Astragalus* and a nutraceutical, exerts different pharmacological effects on the respiratory system. Its anti-inflammatory effects are mediated through numerous signaling pathways (24). A previous study demonstrated that treatment with APS decreased the sneezing and rubbing times of guinea pigs with allergic rhinitis (AR) and hindered the OVA-sIgE, OVA-sIgG1, TNF-α and IL-6 levels in guinea pig serum; it simultaneously elevated the CD25+Foxp3+Treg cell proportion, whereas it decreased the proportion of CD4+IL17+Th17 cells in serum or tissues of guinea pigs with AR, in a dose-dependent manner (25). NF-κB was highly expressed in guinea pigs with AR and its expression was decreased following treatment with APS. NF-κB overexpression stimulated inflammatory responses and Treg/Th17 imbalance in AR guinea pigs. APS decreased the Treg/Th17 imbalance by hindering NF-κB expression, which thus ameliorated the inflammatory responses in guinea pigs with AR (25).

In conclusion, the present study explored the mechanisms of action of APS in improving the immunity of asthmatic mice on the basis of the gut microbiota combined with metabolomics. According to the findings of the present study, APS not only improved the gut microbial imbalance in asthmatic mice, but also exerted its effect by regulating the biosynthesis of unsaturated fatty acids, the biosynthesis of arginine and the pyrimidine-related metabolites. Moreover, the obtained results provide the theoretical foundation for the reasonable application of APS in the clinical treatment of asthma.

Availability of data and materials

The datasets used and/or analyzed during the current study are available from the corresponding author on reasonable request. All sequences used in the present study are publicly available at the NCBI Sequence Read Archive (https://www.ncbi.nlm.nih.gov/bioproject/PRJNA1162806) under the Accession ID PRJNA1162806. The metabolomics data reported in the present study have been deposited in the OMIX, China National Center for Bioinformation/Beijing Institute of Genomics, Chinese Academy of Sciences (https://ngdc.cncb.ac.cn/omix/release/OMIX007407).

Authors' contributions

JZ and MG designed the experiments. JZ, MG, WS and SW performed the experiments. MG and JZ analyzed the data. JZ and MG wrote the manuscript. All authors have read and approved the final manuscript, JZ and WS confirm the authenticity of all the raw data.

Ethics approval and consent to participate

All experimental protocols involving animals were approved by the Ethics Committee of the Zhejiang Center

of Laboratory Animals (Hangzhou, China; approval no. ZJCLA-IACUC-20020187) and conducted conforming to the guidelines of the China Animal Protection Commission.

Patient consent for publication

Not applicable.

Competing interests

The authors declare that they have no competing interests.

References

1. Sun J, Bai S, Zhao J, Li D, Ma X, Ma L and Su X: Mapping knowledge structure and research of the biologic treatment of asthma: A bibliometric study. Front Immunol 14: 1034755, 2023.
2. Agusti A, Fabbri L, Lahousse L, Singh D and Papi A: Single inhaler triple therapy (SITT) in asthma: Systematic review and practice implications. Allergy 77: 1105-1113, 2022.
3. Chan HL and Ng T: Traditional Chinese Medicine (TCM) and allergic diseases. Curr Allergy Asthma Rep 20: 67, 2020.
4. Yang N and Shang YX: Epigallocatechin gallate ameliorates airway inflammation by regulating Treg/Th17 imbalance in an asthmatic mouse model. Int Immunopharmacol 72: 422-428, 2019.
5. Zheng Y, Ren W, Zhang L, Zhang Y, Liu D and Liu Y: A review of the pharmacological action of *Astragalus* polysaccharide. Front Pharmacol 11: 349, 2020.
6. Zhao X, Hu M, Zhou H, Yang Y, Shen S, You Y and Xue Z: The role of gut microbiome in the complex relationship between respiratory tract infection and asthma. Front Microbiol 14: 1219942, 2023.
7. Chen J, Wang A and Wang Q: Dysbiosis of the gut microbiome is a risk factor for osteoarthritis in older female adults: A case control study. BMC bioinformatics 22: 299, 2021.
8. Zhang D, Li S, Wang N, Tan HY, Zhang Z and Feng Y: The Cross-Talk Between Gut microbiota and lungs in common lung diseases. Front Microbiol 11: 301, 2020.
9. Hansen AW and Venkatachalam KV: Sulfur-Element containing metabolic pathways in human health and crosstalk with the microbiome. Biochem Biophys Rep 35: 101529, 2023.
10. Brown HN, Barber T, Renshaw D, Farnaud S, Oduro-Donkor D and Turner MC: Associations between the gut microbiome and metabolic, inflammatory, and appetitive effects of sleeve gastrectomy. Obes Rev 24: e13600, 2023.
11. Arrieta MC, Stiemsma LT, Dimitriu PA, Thorson L, Russell S, Yurist-Doutsch S, Kuzeljevic B, Gold MJ, Britton HM, Lefebvre DL, *et al*: Early infancy microbial and metabolic alterations affect risk of childhood asthma. Sci Transl Med 7: 307ra152, 2015.
12. Li R, Guo Q, Zhao J, Kang W, Lu R, Long Z, Huang L, Chen Y, Zhao A, Wu J, *et al*: Assessing causal relationships between gut microbiota and asthma: evidence from two sample Mendelian randomization analysis. Front Immunol 14: 1148684, 2023.
13. Luo X, Pan Z, Luo S, Liu Q, Huang S, Yang G, Nong F, Fu Y, Deng X and Zhou L: Effects of ceftriaxone-induced intestinal dysbacteriosis on regulatory T cells validated by anaphylactic mice. Int Immunopharmacol 60: 221-227, 2018.
14. Loo EX, Llanora GV, Lu Q, Aw MM, Lee BW and Shek LP: Supplementation with probiotics in the first 6 months of life did not protect against eczema and allergy in at-risk Asian infants: a 5-year follow-up. Int Arch Allergy Immunol 163: 25-28, 2014.
15. Wang F, Wu F, Chen H and Tang B: The effect of probiotics in the prevention of atopic dermatitis in children: A systematic review and meta-analysis. Transl Pediatr 12: 731-748, 2023.
16. Cavalcanti RFP, Gadelha FAAF, Paiva Ferreira LKD, Paiva Ferreira LAM, Chaves Júnior JV, de Araújo Batista RS, Melo TBL, de Souza FS, Alves AF, Maria Batista L and Piuvezam MR: Limosilactobacillus fermentum modulates the gut-airway axis by improving the immune response through FOXP3 activation on combined allergic rhinitis and asthma syndrome (CARAS). Immunobiology 228: 152721, 2023.
17. Dou M, Chu Y, Zhou X, Wang M, Li X, Ma R, Fan Z, Zhao X, Wang W, Li S, *et al*: Matrine mediated immune protection in MS by regulating gut microbiota and production of SCFAs. Mol Neurobiol 61: 74-90, 2024.
18. Hou Q, Huang J, Zhao L, Pan X, Liao C, Jiang Q, Lei J, Guo F, Cui J, Guo Y and Zhang B: Dietary genistein increases microbiota-derived short chain fatty acid levels, modulates homeostasis of the aging gut, and extends healthspan and lifespan. Pharmacol Res 188: 106676, 2023.
19. Tweeddale H, Notley-McRobb L and Ferenci T: Assessing the effect of reactive oxygen species on Escherichia coli using a metabolome approach. Redox Rep 4: 237-241, 1999.
20. Shah SH, Kraus WE and Newgard CB: Metabolomic profiling for the identification of novel biomarkers and mechanisms related to common cardiovascular diseases: Form and function. Circulation 126: 1110-1120, 2012.
21. Robinson O and Lau CE: How do metabolic processes age: Evidence from human metabolomic studies. Curr Opin Chem Biol 76: 102360, 2023.
22. Yao Y, Wang X, Guan J, Xie C, Zhang H, Yang J, Luo Y, Chen L, Zhao M, Huo B, *et al*: Metabolomic differentiation of benign vs malignant pulmonary nodules with high specificity via high-resolution mass spectrometry analysis of patient sera. Nat Commun 14: 2339, 2023.
23. Bjerrum JT, Nielsen OH, Wang YL and Olsen J: Technology insight: metabonomics in gastroenterology-basic principles and potential clinical applications. Nat Clin Pract Gastroenterol Hepatol 5: 332-343, 2008.
24. Xu J, Zhang Q, Li Z, Gao Y, Pang Z, Wu Y, Li G, Lu D, Zhang L and Li D: *Astragalus* polysaccharides attenuate ovalbumin-induced allergic rhinitis in rats by inhibiting NLRP3 inflammasome activation and NOD2-Mediated NF-κB activation. J Med Food 24: 1-9, 2021.
25. He X, Liu L, Luo X, Zhu J, Yang H, Wang J, Chen L and Zhong L: *Astragalus* polysaccharide relieves inflammatory responses in guinea pigs with allergic rhinitis via ameliorating NF-kB-Mediated Treg/Th17 Imbalance. Am J Rhinol Allergy 36: 638-648, 2022.